

Endosome–mitochondria juxtaposition during apoptosis induced by *H. pylori* VacA

F Calore^{1,2}, C Genisset², A Casellato¹, M Rossato³, G Codolo¹, MD Esposti⁴, L Scorrano^{*,1,5,6} and M de Bernard^{*,1,7}

The vacuolating cytotoxin (VacA) is an important virulence factor of *Helicobacter pylori* with pleiotropic effects on mammalian cells, including the ability to trigger mitochondria-dependent apoptosis. However, the mechanism by which VacA exerts its apoptotic function is unclear. Using a genetic approach, in this study we show that killing by VacA requires the proapoptotic Bcl-2 family members BAX and BAK at the mitochondrial level, but not adequate endoplasmic reticulum Ca²⁺ levels, similarly controlled by BAX and BAK. A combination of subcellular fractionation and imaging shows that wild-type VacA, but not mutants in its channel-forming region, induces the accumulation of BAX on endosomes and endosome–mitochondria juxtaposition that precedes the retrieval of active BAX on mitochondria. It is noteworthy that in *Bax-* and *Bak-*deficient cells, VacA is unable to cause endosome–mitochondria juxtaposition and is not retrieved in mitochondria. Thus, VacA causes BAX/BAK-dependent juxtaposition of endosomes and mitochondria early in the process of cell death, revealing a new function for these proapoptotic proteins in the regulation of relative position of organelles.

Cell Death and Differentiation (2010) 17, 1707–1716; doi:10.1038/cdd.2010.42; published online 30 April 2010

The vacuolating cytotoxin A (VacA) is one of the major virulence factors produced by *Helicobacter pylori*, the Gram-negative bacterium that infects > 50% of the human population. *H. pylori* causes peptic ulcer disease and is an early risk factor for gastric cancer.¹ VacA is not only the toxin responsible for vacuolization of cells exposed to *H. pylori* culture filtrates,² but also shows pleiotropic effects on mammalian cells.^{3,4} VacA is produced as a 140 kDa precursor, which is cleaved during secretion from the bacterium into a 87–95 kDa mature toxin. The latter can be further cleaved into an amino-terminal p37 domain and a carboxy-terminal p58 domain, which remain noncovalently linked. Secreted VacA is a flower-shaped oligomer, formed by six or seven monomers. After a short exposure to acidic or basic pH, the oligomer is disassembled and VacA becomes able to interact with lipid bilayers. Interaction with biological membranes triggers restoration of the oligomers to form anion-selective, voltage-dependent channels.⁵ The membrane channel-forming ability of VacA resides in its amino-terminal portion, and single amino acid substitutions (P9A and G14A) in the p37 domain completely abrogate it.^{6,7} Vacuolization of epithelial cells by VacA is strictly dependent on the formation of anion-selective membrane channels, which are

targeted to late endosomes after internalization of the toxin.^{3,5,8,9} Indeed, once bound to the cell surface, VacA is rapidly internalized by a pinocytotic mechanism that involves F-actin but is independent of clathrin, dynamin, and of the ARF6 GTPase. It is then routed to early endosomes before reaching late endosomes.^{10,11}

H. pylori has been associated with increased level of apoptosis in human gastric mucosa.^{12–15} It has been proposed that loss of specialized cells (especially the gastric parietal cells) resulted in alterations of crucial cellular cross-talk pathways, eventually leading to disturbed differentiation and to the initiation of the metaplasia/dysplasia/carcinoma sequence.¹⁶ Although multiple *H. pylori* factors, including products of *cag* pathogenicity island¹⁷ and lipopolysaccharide,¹⁸ are likely to be involved, VacA is *per se* sufficient to induce cell death.^{19,20}

Apoptosis is a genetically controlled, evolutionarily conserved pathway in which intracellular organelles have a major regulatory role. Mitochondria, in particular, integrate and amplify diverse apoptotic signals by releasing into the cytosol (Cyt) cytochrome *c* and other cofactors required for the activation of the effector caspases, which then dismantle the cellular structures. The release of cytochrome *c* is controlled

¹Venetian Institute of Molecular Medicine, V. Orus 2, Padova 35129, Italy; ²Department of Biomedical Sciences, University of Padova, V.G. Colombo 3, Padova 35121, Italy; ³Division of General Pathology, Department of Pathology, University of Verona, Strada Le Grazie 8, Verona 37134, Italy; ⁴Faculty of Life Sciences, University of Manchester, Oxford Road M13, Manchester 9PT, UK; ⁵Dulbecco-Telethon Institute, Via Orus 2, Padova 35129, Italy; ⁶Department of Cell Physiology and Metabolism, University of Geneva Medical School, 1 Rue M. Servet, Genève 1211, Switzerland and ⁷Department of Biology, University of Padova, Via U. Bassi 58/B, Padova 35121, Italy

*Corresponding author: M de Bernard, Department of Biology, University of Padova, Venetian Institute of Molecular Medicine, Via Orus 2, Padova 35129, Italy. Tel: +39 049 792 3223; Fax: +39 049 792 3250; E-mail: marina.debernard@unipd.it or

Luca Scorrano, Dulbecco-Telethon Institute, Via Orus 2, Padova 35129, Italy. Tel: +39 049 792 3221; Fax: +39 049 792 3271; E-mail: lscorrano@dti.telethon.it

Keywords: *Helicobacter pylori*; VacA; apoptosis; mitochondria; BAX

Abbreviations: Cyt, cytosol; CS, culture supernatant; DKO, double knockout; ER, endoplasmic reticulum; MEF, mouse embryonic fibroblast; Mt, mitochondria; mtBAX, mitochondria-targeted BAX; NP, nuclear pellet; PNS, post nuclear supernatant; SERCA, sarco/endoplasmic reticulum Ca²⁺-ATPase; VacA, vacuolating cytotoxin A; wt, wild-type; mtRFP, red fluorescent protein targeted to mitochondria; LBPA, lysobisphosphatidic acid; DMEM, Dulbecco's modified Eagle's medium; BSA, bovine serum albumin; FITC, fluorescein isothiocyanate; TRITC, tetramethyl rhodamine isothiocyanate; GFP, green fluorescence protein; IRES, internal ribosomal entry site
Received 21.9.09; revised 12.2.10; accepted 30.3.10; Edited by G Melino; published online 30.4.10

by BCL-2 family members, which include both anti- and pro-apoptotic proteins. In a widely accepted model, the so-called 'BH3-only' proapoptotic members of the family sense the damage signal and transmit it to the so-called 'multidomain proapoptotics' BAX and BAK, which are required for the activation of the mitochondrial pathway of apoptosis. Once activated by BH3-only proteins, BAX and BAK provide a physical pathway for the efflux of cytochrome *c* from mitochondria. In addition, they dictate steady-state Ca^{2+} levels in the endoplasmic reticulum (ER), thus controlling the response to Ca^{2+} -mediated death stimuli.²¹

Apoptosis induced by VacA might follow the activation of the mitochondrial pathway of apoptosis, as suggested by the ability of VacA to lower mitochondrial membrane potential ($\Delta\psi_m$)²² and to release cytochrome *c*.²³ Accordingly, both a fusion protein between the N-terminal fragment of VacA (p37) and GFP, and the purified toxin, localize to mitochondria.²⁴ Loss of $\Delta\psi_m$ and cytochrome *c* release require the channel-forming domain of VacA.^{7,24,25} This led to the hypothesis that $\Delta\psi_m$ dissipation and/or cytochrome *c* release were a direct consequence of a VacA channel in the mitochondrial inner membrane, independently from host factors.²⁶ However, VacA activates the multidomain proapoptotic proteins BAX and BAK before the release of cytochrome *c*.²⁷ This complicates the picture and leaves us with a number of open questions: Is VacA targeted to mitochondria? How? Does it require BAX and BAK to kill? Does it rely on adequate ER Ca^{2+} levels or on the direct mitochondrial function of BAX and BAK?

In this study we used a genetic approach to investigate the mechanisms of apoptosis induced by VacA. VacA requires BAX and BAK at the mitochondrial level to kill. Unexpectedly, active VacA also induces the translocation of BAX to endosomes, in parallel with the co-segregation of endosomal and mitochondrial membranes. Co-segregation and cell death strictly depend on the channel-forming domain of the toxin and on the presence of BAX and BAK. Thus, the program of VacA-induced apoptosis includes an unexpected subroutine of BAX- and BAK-dependent endosomal juxtaposition to mitochondria, extending the known roles of these proapoptotic proteins.

Results

Apoptosis by VacA requires integrity of its channel-forming domain and BAX and BAK. We evaluated whether apoptosis induced by *H. pylori* culture supernatant (CS) in mouse embryonic fibroblasts (MEFs) required the multidomain proapoptotics BAX and BAK. MEFs doubly deficient for *Bax* and *Bak* (double knockout (DKO))²⁸ were resistant to apoptosis induced by the *H. pylori* supernatant when compared with their wild-type (wt) counterparts (Figures 1a and b). We then verified whether apoptosis occurring in wt cells required the channel-forming activity of VacA. CS obtained from two isogenic mutants of *H. pylori* carrying a point mutation in the *VacA* gene (P9A and G14A) that renders the toxin unable of forming anion channels^{7,29} were greatly ineffective in inducing cell death (Figure 1a and Supplementary Figure 1a). When we measured

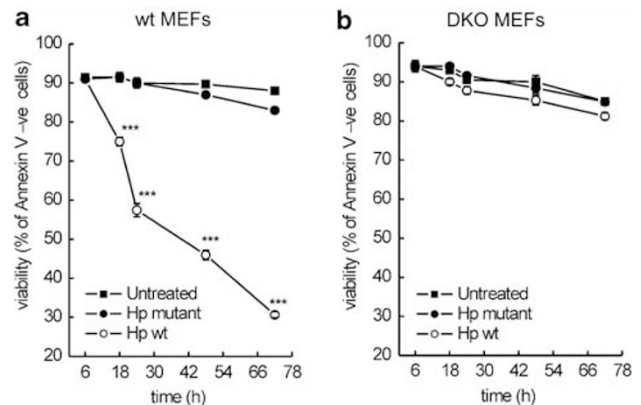


Figure 1 VacA-induced cell death requires proapoptotic proteins BAX and BAK. (a) Wt MEF cells were incubated with *H. pylori* CS, either wt or P9A mutant. After 6, 18, 24, 48 and 72 h, the Annexin-V assay was performed following the manufacturer's instructions. Viability was determined cytofluorimetrically as the percentage of Annexin-V-Alexa 568-negative cells. (b) *Bax/Bak* DKO MEF cells were incubated and assayed for viability as above. Cells not exposed to *H. pylori* CS are defined as untreated cells. Data represent mean \pm S.D. of 20 independent experiments. Significance was determined using Student's *t*-test for paired data of CS-intoxicated cells versus untreated cells; ****P* < 0.01

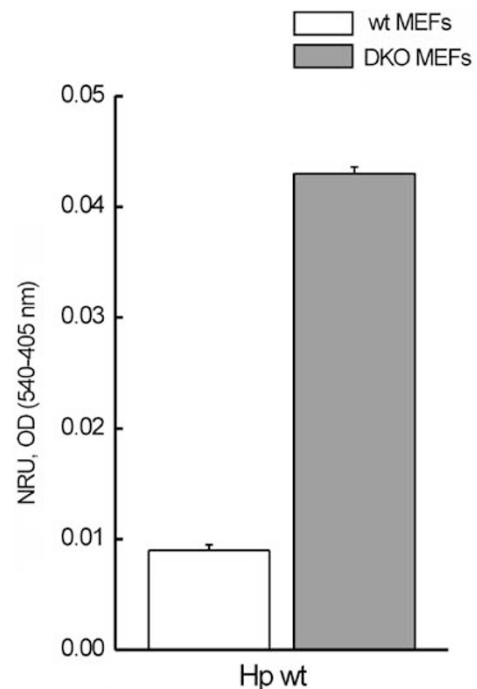


Figure 2 VacA induces vacuolization in DKO, but not in wt MEFs. Wt and DKO MEFs were incubated with *H. pylori* wt CS. After 5 h, the extent of vacuolization was measured by neutral red uptake assay. Results are expressed as difference between the OD values obtained at 540 and 405 nm and are the mean \pm S.D. of three independent experiments

vacuolization of wt and DKO MEFs in response to the CS of *H. pylori* wt, we found that DKO cells were much more responsive, reaching maximal vacuolization after 5 h (Figure 2), whereas wt cells showed little or no vacuolization until 24 h (not shown). As expected, DKO

cells did not vacuolate after exposing to the CS of the *H. pylori* mutant strain (not shown). Thus, vacuolization and apoptosis seem to be independent, with the former even stimulated by the lack of BAX and BAK. In conclusion, the proapoptotic proteins BAX and BAK are required for VacA-induced apoptosis, which relies on its VacA channel properties.

VacA-induced apoptosis involves BAX-dependent regulation at the mitochondrial level. As BAX and BAK regulate apoptosis at multiple levels,³⁰ we reasoned that the insensitivity of DKO cells to VacA-induced apoptosis could reflect their downregulation of Ca^{2+} levels in the ER. To test this possibility, we turned to a model of DKO MEFs whose multiple defects were genetically and selectively corrected: the mitochondrial one by targeting BAX exclusively to mitochondria, and the ER one by overexpressing sarco/endoplasmic reticulum Ca^{2+} -ATPase (SERCA),³⁰ the Ca^{2+} -ATPase responsible for the uptake of Ca^{2+} from the Cyt into the ER lumen.³¹ Expression of mitochondria-targeted BAX (mtBAX) restored the sensitivity of DKO MEF cells to VacA-induced apoptosis, although cells remained more viable than their wt counterparts (compare Figure 3a with 1a), probably because of the lack of BAK. Conversely, the overexpression of SERCA had no effect (Figure 3b). This indicates that VacA falls into the category of stimuli that require mitochondria-based multidomain proapoptotics and can proceed despite depleted intracellular Ca^{2+} stores. As expected, CS from the *H. pylori* VacA P9A channel mutant was also unable to trigger apoptosis in mtBAX-corrected DKO cells. In conclusion, VacA recruits the so-called 'mitochondrial gateway' of apoptosis to kill intoxicated cells.

VacA induces BAX activation and its recruitment to mitochondria. In resting cells the multidomain proapoptotic protein BAX resides as a monomer in the Cyt or is loosely

attached to intracellular membranes. Once cells are stressed by an apoptotic stimulus, BAX becomes active, exposes its C-terminal α -9 helix, and translocates to mitochondria.^{32–34} This conformational change can be monitored by following the exposure of new epitopes using specific antibodies. The wt *H. pylori* CS induced BAX activation and the parallel staining with anti-VacA antibodies revealed a partial, but significant, colocalization between the two proteins (Figure 4a). No BAX activation was observed after administering the CS of the mutant strain, again underlining the central role of the VacA channel-forming activity. The weaker VacA staining observed in the latter case was probably because of a less efficient entry of the toxin into the cell. We therefore waited until 48 h, when the staining of VacA increased; yet, BAX did not become activated (not shown). Furthermore, mitochondria purified from cells incubated for 24 h with wt CS revealed a clearcut recruitment of BAX that was completely absent in untreated cells or in cells exposed to the mutant strain (Figure 4b). This was not a consequence of an increase in total BAX, as measured by specific immunoblotting in lysates of cell exposed to wt and mutant CS (data not shown).

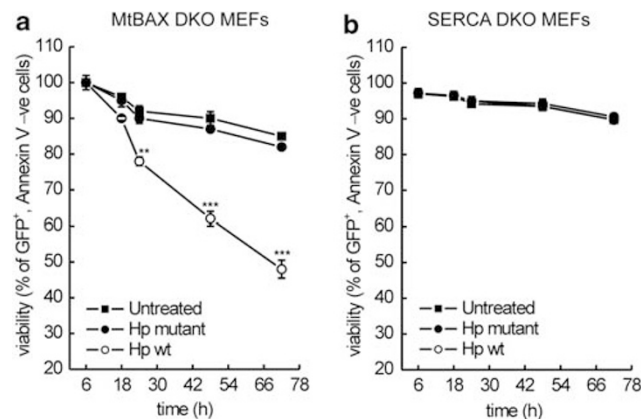


Figure 3 VacA-induced cell death involves the mitochondrial apoptotic gateway. DKO MEF cells were genetically and selectively corrected: the mitochondrial defect by targeting BAX exclusively to mitochondria (a), and the ER defect by overexpressing SERCA (b). Cells were incubated and assayed for viability as in Figure 1. Cells not exposed to *H. pylori* CS are defined as untreated cells. Data represent mean \pm S.D. of 20 independent experiments. Significance was determined using Student's *t*-test for paired data of CS-intoxicated cells versus untreated cells; ***P* < 0.02; ****P* < 0.01

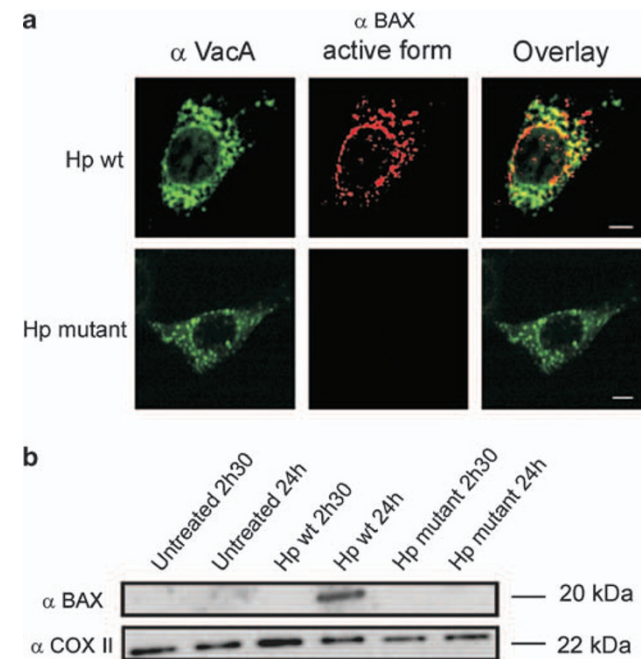


Figure 4 VacA triggers BAX activation and its translocation to mitochondria. (a) Representative confocal images of wt MEF cells incubated for 24 h with *H. pylori* CS, either wt or P9A mutant. Cells were immunostained with a rabbit anti-VacA antibody and a secondary FITC anti-rabbit antibody. BAX was detected with a murine monoclonal primary antibody specific for its activated form (clone 6A7) and a secondary TRITC anti-mouse antibody. The images are representative of 60 cells examined from five separate experiments. Scale bars: 10 μ m. Mander's coefficient for VacA and activated BAX colocalization was 0.21 ± 0.0231 in wt *H. pylori* CS-intoxicated cells versus 0.09 ± 0.00198 in P9A mutant CS-treated ones (*n* = 5 independent experiments, 60 cells per experiment). (b) Mitochondria were purified from wt MEF cells incubated with wt or P9A mutant *H. pylori* supernatants for the indicated time points; 15 μ g of mitochondrial proteins were separated by SDS-PAGE and immunoblotted; BAX was revealed with a rabbit anti-BAX antibody. An anti-COX II monoclonal antibody was used as control for equal loading. Cells not exposed to *H. pylori* CS are defined as untreated cells

The channel-forming region of VacA is required for its localization to mitochondria. Whether VacA is targeted to mitochondria during apoptosis, or is retained in late endosomes, remains an open question.^{23,24,27} Given the requirement of the mitochondrial gateway to induce apoptosis, we investigated the subcellular localization of VacA from its entry into the cell to the induction of apoptosis. In a preliminary set of experiments we verified that our subcellular fractionation of cells yielded pure mitochondrial and early and late endosomal fractions (Figure 5). We therefore monitored by immunoblotting the accumulation of VacA in purified mitochondrial and early and late endosomal subcellular fractions from cells incubated for 24 h with wt or with VacA P9A *H. pylori* CS. Wt VacA was present in both endosomal compartments, as expected for a toxin that enters the cells by endocytosis, and interestingly, in part also in the mitochondrial fraction (Figure 6a). Conversely, VacA P9A accumulated in endosomal compartments without reaching

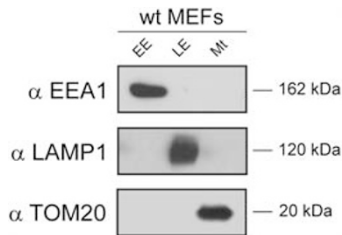


Figure 5 Distribution of EEA1, LAMP1 and TOM20 in endosomal and mitochondrial fractions purified from wt MEF cells. early endosomes (EE), late endosomes (LE) and mitochondria were separated as described and 15 μ g of protein was separated by SDS-PAGE and immunoblotted with the indicated antibodies

mitochondria (Figure 6a). Moreover, the mutated toxin was internalized less efficiently than the wt one, despite a similar concentration in the CS (not shown). A gel overloaded with endosomal and mitochondrial proteins, purified from VacA P9A-intoxicated cells, permitted to exclude that the absence of the protein in mitochondrial fraction was because of its less efficient internalization (Figure 6a). The role of the channel activity of VacA in its targeting to mitochondria was further confirmed by applying to the cells the other channel-defective mutant, VacA G14A;⁷ it accumulated in endosomes as well as the wt counterpart, but it did not reach mitochondria (Supplementary Figure 1b). We further confirmed the subcellular localization of VacA by confocal microscopy using anti-VacA antibodies in MEFs expressing a mitochondrially targeted red fluorescent protein. Although in cells treated with the mutated VacA the distribution of the toxin-positive vesicles was clearly distinct from that of mitochondria, in cells incubated for 24 h with wt VacA several toxin-positive spots appeared closely apposed to mitochondria (Figure 6b). Thus, association of VacA with mitochondria seems to require the same domain involved in channel formation.

In VacA-intoxicated cells, endosomes are juxtaposed to mitochondria. Our previous experiments left open the question of how VacA transited from endosomes to mitochondria, leading to BAX activation. We therefore decided to follow the subcellular localization of VacA in infected wt and DKO cells in parallel with BAX activation in the former. The wt toxin accumulated in the endosomal fractions as early as 2 h and 30 min after infection, although a small portion of the protein was already detectable in the

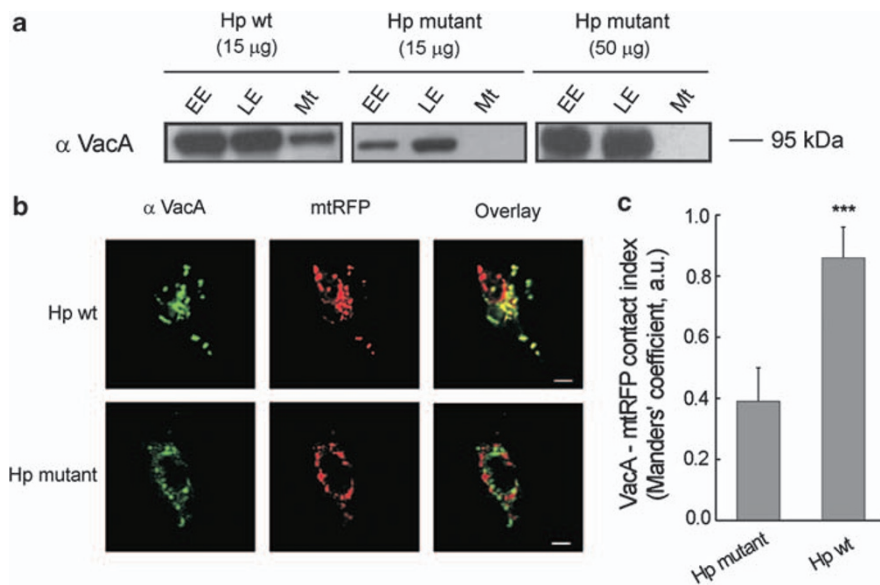


Figure 6 VacA targets mitochondria. (a) Wt MEF cells were incubated for 24 h with wt or P9A mutant *H. pylori* supernatants, harvested and subfractionated as described. Fifteen or 50 μ g of early endosomal (EE), late endosomal (LE) and mitochondrial (Mt) proteins were separated by SDS-PAGE and immunoblotted using the indicated antibody. (b) Wt MEF cells, transfected with plasmid encoding for mtRFP, were incubated with wt or P9A mutant *H. pylori* CS. After 24 h of incubation, cells were fixed and the toxin was stained with a rabbit anti-VacA antibody followed by a secondary FITC anti-rabbit antibody. Images are representative of 60 cells examined from three separate experiments. Scale bars, 10 μ m. (c) Mean \pm S.D. ($n = 3$, 20 cells per independent experiment) of colocalization data from b. Significance was determined using Student's *t*-test for paired data of wt *H. pylori* CS-treated versus P9A *H. pylori* CS-treated cells; *** $P < 0.01$

mitochondrial fraction. After 12 h, wt VacA was extensively retrieved in the mitochondrial fraction, whereas endosomes exclusively remained positive for the mutated toxin (devoid of channel activity). Unexpectedly, in cells treated with the active *H. pylori* CS, after as soon as 2 h and 30 min, BAX was retrieved in the early endosomes fraction, devoid of contamination by Cyt, as confirmed by the absence of the cytosolic marker GAPDH (Supplementary Figure 2b). The major proportion of BAX recruited on endosomes was not membrane integral, as confirmed by its sensitivity to alkali extraction (Supplementary Figure 2a). Notably, no recruitment of active BAX was detected on endosomal and mitochondrial fractions in cells exposed to mutated VacA, as well as in untreated cells (Figure 7). Furthermore, wt VacA induced a progressive accumulation of early (EEA1) and late (LAMP1) endosomal markers in the mitochondrial fraction (Figure 7). In contrast, when cells were incubated with the mutant in the channel-forming region of VacA (P9A mutant), both markers were confined to their correspondent fraction and did not co-purify with mitochondria (Figure 7). Similarly, neither endosomal markers nor BAX were found associated with mitochondria in cells exposed to the other channel-defective mutant, VacA G14A (Figure 8a). Importantly, the

endosomal fractions of wt VacA-treated cells were not positive for a mitochondrial marker (Figure 8b), indicating that the retrieval of BAX in endosomes was not an epiphenomenon of the accumulation of mitochondrial fragments within the endosomal fraction. Thus, VacA induces a major alteration in vesicular traffic that results in co-segregation of early and late endosomes with mitochondria, a situation similar to that reported in Fas-activated T cells.³⁵ This early alteration occurs around the same time as the accumulation of active BAX in the early endosomes fraction, well before its retrieval on mitochondria. It is noteworthy that no endosomal recruitment of the already mitochondrial BAK was observed (not shown).

Significant amounts of VacA accumulate in the mitochondrial fraction after 12 h of intoxication (Figure 7), when apoptosis is still not measurable, suggesting that targeting precedes induction of death. To confirm this, we turned to DKO cells, in which we expected to recapitulate the targeting to mitochondria of VacA and their cofractionation with endosomes, in the complete absence of apoptosis. Surprisingly, in these cells VacA did not colocalize at all with mitochondrial markers, nor it induced a co-segregation of endosomal and mitochondrial membranes within 12 h of intoxication (Figure 7). At 24 h, a small portion of VacA appeared to be targeted to mitochondria, even if endosomal markers did not reach the mitochondrial fraction.

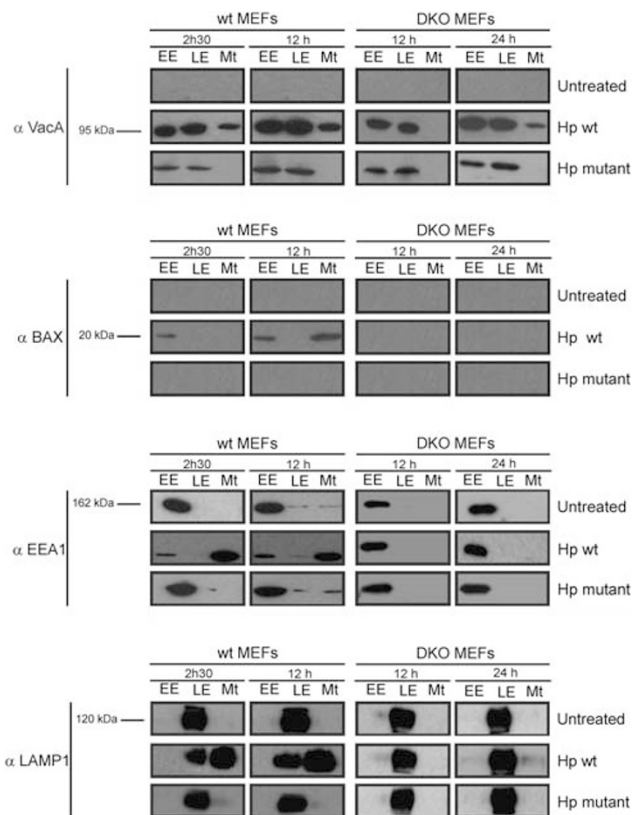


Figure 7 VacA induces co-segregation of endosomal and mitochondrial membranes. Wt or DKO MEF cells were incubated with *H. pylori* CS, either wt or P9A mutant; at the indicated time points subcellular fractionation was performed and 15 μ g of early endosomal (EE), late endosomal (LE) and mitochondrial (Mt) proteins were separated by SDS-PAGE and immunoblotted; VacA, BAX, EEA1 and LAMP1 were revealed by specific antibodies. Cells not exposed to *H. pylori* CS are defined as untreated cells

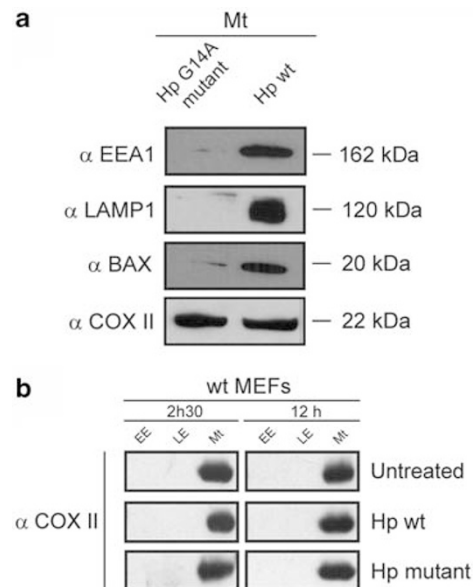


Figure 8 (a) VacA G14A does not induce endosomal hijack on mitochondria. Mitochondria were purified from cells intoxicated for 24 h with *H. pylori* CS (either wt or G14A mutant). Using SDS-PAGE, 15 μ g of proteins were then separated and membranes were probed with polyclonal anti-EEA1, anti-LAMP1 and anti-BAX antibodies. COX II was used as marker of equal loading for mitochondria. (b) Distribution of COX II in endosomal and mitochondrial fractions purified from intoxicated wt MEFs. A total of 15 μ g of early endosome (EE), late endosome (LE) and mitochondria (Mt) proteins purified from wt MEF cells untreated, treated with wt *H. pylori* CS, or with the mutant P9A one, were loaded in SDS-PAGE and immunoblotted. The exclusive localization of COX II in mitochondria permits to exclude any contamination of endosomes by fragment of mitochondria during the subcellular fractionation

We wished to confirm that mitochondria and endosomes become closer in cells intoxicated with VacA. Immunofluorescence analysis of cells exposed to VacA further substantiated the ability of the wt toxin to promote juxtaposition between early/late endosomes and mitochondria (Figure 9), and suggested an association of endosomal vesicles (containing VacA) with mitochondria. It is noteworthy that the relocalization of endosomes in proximity to mitochondria was not observed in cells exposed to intrinsic or extrinsic apoptotic stimuli, such as staurosporine, etoposide and TNF- α (Supplementary Figure 3). This suggests that juxtaposition of endosome to mitochondria occurs specifically in cell exposed to VacA and is not a general feature of apoptosis.

Immunoelectron microscopy analysis performed on intoxicated MEF cells further corroborated this finding. Intoxication of wt MEFs with CS from *H. pylori* wt strain, but not from the mutant one, for 2 h and 30 min triggered the juxtaposition of endosomal compartments (positive to the late endosomal marker lysobisphosphatidic acid (LBPA)) to mitochondria (Figure 10a and see quantification in b). At the same time, endosomal area remained the same in wt VacA-intoxicated and untreated cells (Figure 10c). Unfortunately, any attempt to visualize early endosome-positive structures failed as a consequence of the very poor immunoreactivity of the EEA1 antibody in our immunoelectron microscopy protocol (not shown).

In conclusion, the combination of subcellular fractionation, imaging and immunoelectron microscopy indicates that in cells intoxicated with VacA, mitochondria and endosomes are in close proximity. Notably, at longer time points the juxtaposition evolves in the engulfment of mitochondria in autophagosomes (not shown).³⁶

Discussion

In this study we report that in cells intoxicated with the *H. pylori* cytotoxin VacA endosomes are retrieved in close proximity to mitochondria, in parallel with the accumulation of the toxin in the latter organelle. The endosomal markers EEA1 (specific for early endosomes) and LAMP1 (more typical of late endosomes) are enriched in the mitochondrial fraction after as early as 2 h and 30 min from intoxication. Hence, the colocalization of VacA with Rab7 reported by Yamasaki *et al.*²⁷ could reflect the same membrane mistargeting as documented here. We suggest that VacA targets mitochondria in virtue of the cross-talk between these organelles that may be enhanced during apoptosis induction.³⁵ In support of this conclusion, in *Bax/Bak* DKO cells that show no accumulation of endosomal markers in mitochondria, VacA remains confined at the endosomal level. The co-segregation of VacA and endosomal markers with mitochondria is not a

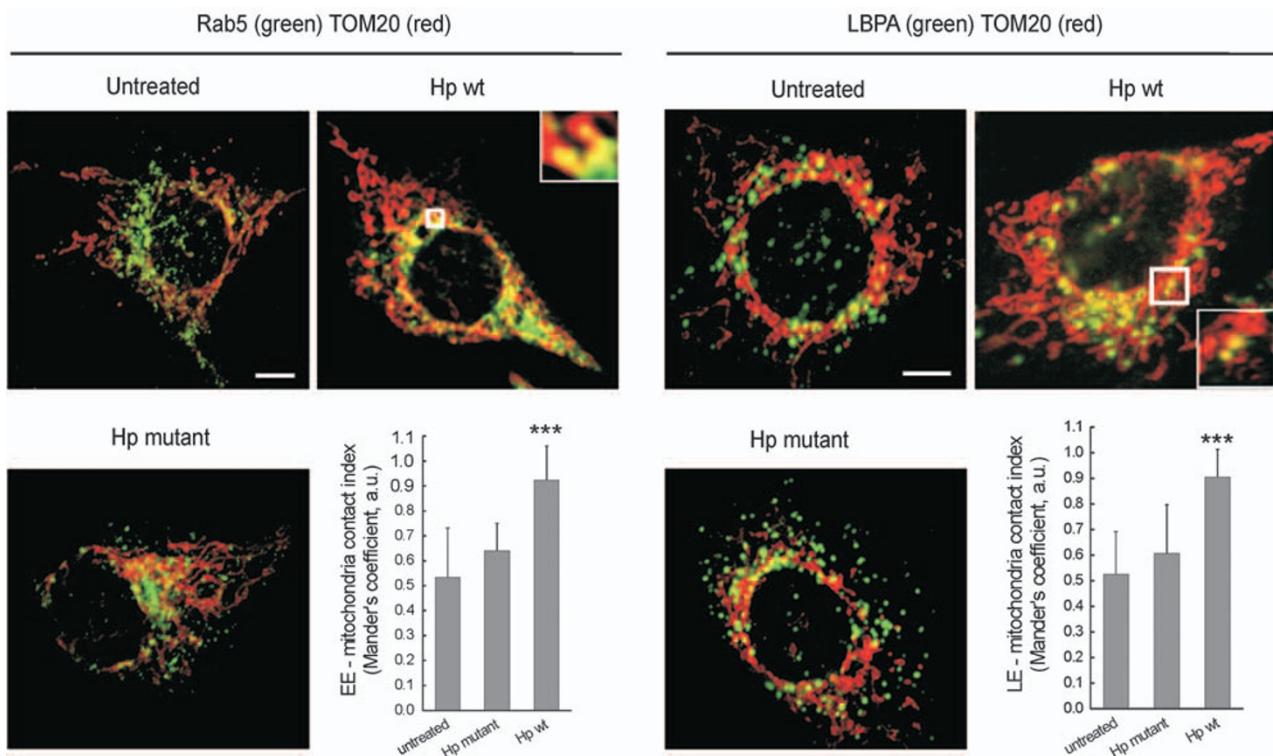


Figure 9 Early and late endosomes are close to mitochondria in VacA-intoxicated cells. Wt MEF cells were incubated for 12 h with *H. pylori* CS, either wt or P9A mutant, before being processed for immunofluorescence. (Left panels) anti-Rab5 (green staining) and anti-TOM20 (red staining) antibodies were used to label early endosomal and mitochondrial membranes, respectively. (Right panels) anti-LBPA (green staining) was used to label late endosomal membranes. Scale bars, 10 μ m. Squares containing a magnification of a detail show the evident colocalization between endosomal and mitochondrial markers in cells exposed to the wt toxin. Cells not exposed to *H. pylori* CS are defined as untreated cells. All these images are representative of 60 cells per condition examined from three separate experiments. Mean \pm S.D. ($n=3$, 20 cells per experiment) of colocalization data are reported. Significance was determined using Student's *t*-test for paired data of wt CS-intoxicated cells versus untreated cells/cells exposed to 326 P9A. *** $P<0.01$

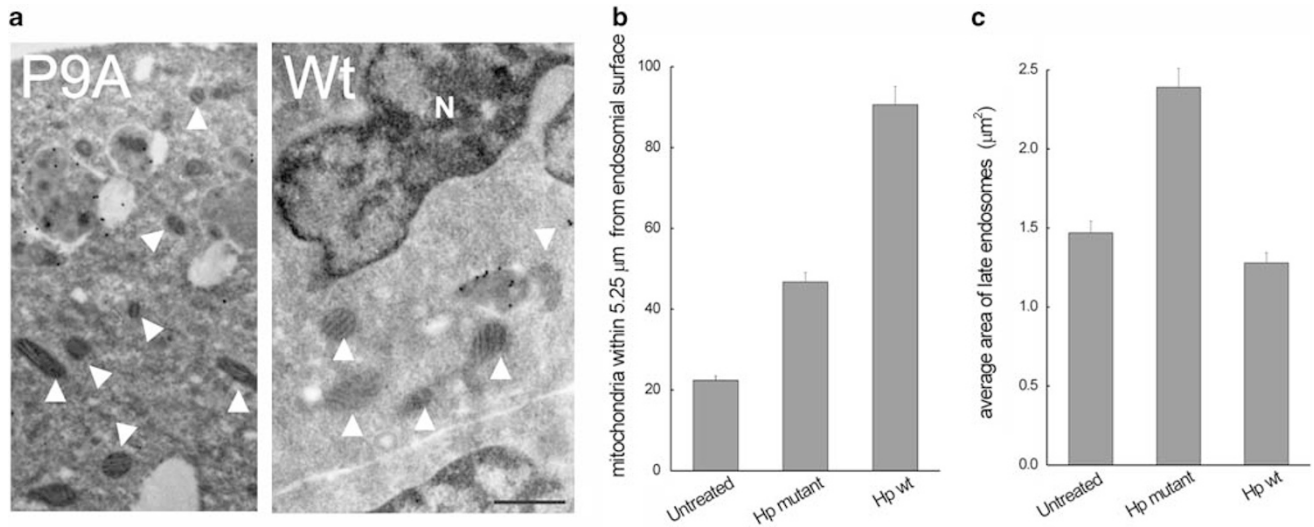


Figure 10 Endosomal membranes cofractionate with mitochondria in cells intoxicated with VacA. Wt MEF cells were incubated for 2 h and 30 min with *H. pylori* CS, either wt or P9A mutant, before being processed for immunoelectron microscopy. (a) anti-LBPA antibody was used to label late endosomal membranes in cells exposed to P9A mutant (left panel) or to wt CS (right panel) respectively. N, nucleus; arrowheads point to mitochondria; gold particles identify late endosomes. Scale bar corresponds to 0.84 μm for the left panel and to 0.47 μm for the right panel. (b) Morphometry analysis of MEF treated and processed as in a. The number of mitochondria located within 5.25 μm from the endosomal surface was counted (22.37 ± 1.1 in untreated cells, 46.74 ± 2.33 in 326 P9A-treated cells and 90.63 ± 4.53 in 326 wt treated cells). Numbers refer to mitochondria identified in a total area of 65 μm² around endosomes. (c) Morphometry analysis of MEF cells treated and processed as in a. The total cell area occupied by late endosomes was measured (an average of 12 endosomes were considered for each condition)

mere consequence of apoptosis induction, because it occurs before any detectable cell death.

Convergent traffic between endosomes and mitochondria has been previously documented in TNF-α-exposed hepatocytes,³⁷ Fas-activated T cells³⁵ and also reticulocytes, in which a direct shuttling of iron from one organelle to the other occurs without any cytosolic intermediary.³⁸ In addition, changes in the intracellular localization of mitochondria and generation of clusters of organelles has been reported in a variety of apoptotic settings.³⁹ Although this inter-organelle membrane traffic may be specific to some cellular contexts, the possibility that such a traffic pathway is constitutively present in other cell types deserves further investigation.

Previous results showed that VacA induced activation of the proapoptotic proteins BAX and BAK.²⁷ However, the main proapoptotic ‘multidomain’ proteins BAX and BAK control not only the physical permeabilization of the outer membrane of mitochondria,²⁸ but also the levels of ER Ca²⁺ and hence the susceptibility to Ca²⁺-dependent death stimuli.³⁰ Our results lend support to a model in which VacA engages the so-called ‘mitochondrial gateway’ of apoptosis. Cells lacking both *Bax* and *Bak* intoxicated with VacA do not die, indicating the requirement of these key mediators of apoptosis in the death by VacA. Re-expression of a BAX mutant exclusively targeted to mitochondria significantly restored cell sensitivity to the toxin, whereas the genetic correction of the reduced ER Ca²⁺ levels of the *Bax*- and *Bak*-deficient cells did not restore their susceptibility to VacA.

During apoptosis BAX can be targeted to different intracellular membranes, from mitochondria to ER to Golgi.⁴⁰ However, to the best of our knowledge, BAX has never been reported to localize on endosomes. More importantly, these

organelles could serve as platforms for BAX recruitment onto mitochondria. Our data would be consistent with two models: (1) BAX is recruited to early endosomes in a VacA-dependent process; BAX activated on endosomal membranes then drags the whole organelles to mitochondria by virtue of its affinity to the outer mitochondrial membrane; and (2) alternatively, although a fraction of BAX is directly recruited to the mitochondrial membrane as a consequence of VacA intoxication, another fraction of BAX reaches the mitochondria through membrane trafficking involving endosomes. This latter model is consistent with the observation that the amount of BAX associated with mitochondria after 12 h of incubation with VacA is significantly greater than would be expected solely from its recruitment after intermixing of mitochondria with endosomes. The selectivity of BAX recruitment to early (rather than late) endosomes is not clear. Co-immunoprecipitation did not reveal any interaction between VacA and the proapoptotic protein. However, this is not indicative that the two proteins do not interact; for example, co-immunoprecipitation between BID and BAX is similarly negative as the interaction occurs in the membrane.⁴¹ This envisions a scenario in which VacA is responsible for the mistargeting of endosomal membranes close to the mitochondria. This seems to be an essential step for accumulation of VacA and BAX in mitochondria, thereby dictating the final amount of this proapoptotic protein accumulated in this organelle during VacA intoxication.

The VacA-induced endosome relocalization, as well as the BAX recruitment onto these organelles, requires the channel-forming domain of VacA; mutations in this region arrested the toxin in late endosomes, abrogated recruitment of BAX to endosomes and mitochondria and eliminated the proapoptotic effect of the toxin.

Surprisingly, DKO cells are much more susceptible to vacuolization after VacA intoxication than their wt counterpart, showing that vacuolization and apoptosis are two genetically distinguishable processes, despite the requirement of channel-forming domain for both. As the different vacuolization does not result from an increased entry of the toxin in DKO cells, it raises the intriguing possibility that BAX and BAK are involved in an intracellular traffic of membranes. In this scenario, the absence of BAX/BAK would result in larger endosomes, explaining the pronounced effect of VacA on size and extent of vacuoles in DKO cells (Supplementary Figure 2). If the constitutive pathway of endosomal remodeling is somehow blunted by the lack of these multidomain proapoptotics, more membranes would be available for vacuolization by VacA. Consistently, VacA is unable to induce the co-fractionation of endosomes and mitochondria in DKO cells.

In conclusion, our work shows that apoptosis induced by VacA requires BAX and BAK and is Ca^{2+} independent. Furthermore, it elucidates the route used by VacA to target mitochondria in the course of apoptosis and indicates an unexpected new function for the key proapoptotic protein BAX in the dynamics of intracellular organelles.

Materials and Methods

Materials. MEFs were cultured as described by Scorrano *et al.*³⁰ Transfection was performed using Transfectin Lipid Reagent (Bio-Rad, Richmond, CA, USA) following the manufacturer's instructions. All chemicals, unless specified, were from Sigma (St. Louis, MO, USA). *H. pylori* G14A strain was provided by Novartis (Siena, Italy). Protease inhibitor cocktail was from Roche (Penzberg, Germany). TNF- α was from Alexis Biochemicals (Lausen, Switzerland). Plasmid pCDNA3.1 encoding a red fluorescent protein targeted to mitochondria (mtRFP) was a gift from M Zaccolo (University of Glasgow, UK). Polyclonal antibody anti-VacA was provided by Novartis; polyclonal antibodies anti-LAMP1 and anti-EEA1 were from Abcam (Cambridge, UK); monoclonal antibody anti-BAX (clone 6A7) was from Biosource (Camarillo, CA, USA); and polyclonal antibody anti-BAX and monoclonal antibody anti-COX II were from Upstate (Lake Placid, NY, USA). Monoclonal and polyclonal antibodies anti-Rab5 were a gift from M Zerial (Max Planck Institute, Berlin, Germany); monoclonal antibody (clone 6C4) anti-LBPA was kindly provided by J Gruenberg (University of Geneva, Switzerland); polyclonal antibody anti-TOM20 was from Santa Cruz Biotechnology, Inc. (Santa Cruz, CA, USA), monoclonal antibody anti-complex II subunit 70 kDa was from MitoSciences (Eugene, OR, USA) and monoclonal antibody anti-GAPDH was from Merck (Nottingham, UK).

Bacteria and culture conditions. *H. pylori* strain SPM 326, which encodes an s1m1-type VacA,⁴² and two isogenic vacA mutant strains carrying the point mutations, P9A²⁹ and G14A,⁷ were maintained in 5% CO₂ at 37°C on Columbia agar plates supplemented with 5% horse blood. Colonies were inoculated into brain heart infusion broth containing 5% FBS and were cultured for 2 days in rotary shaking at 180 r.p.m. at 37°C under microaerophilic conditions.

Proteins of supernatant from broth culture, diluted to an optical density at 600 nm (OD₆₀₀) of 0.8, were precipitated with 50% ammonium sulfate and resuspended in 20 mM Hepes pH 7.4 in 1/15 of the initial volume as described by Skibinski *et al.*⁴³ Concentrated supernatants were dialysed against the same buffer. A western blot analysis carried on the bacterial supernatant from either wt or from the mutant *H. pylori* strain revealed that the toxin content was equivalent between the two preparations and accounted for approximately 4% of the total protein.

Cell intoxication. For all the experiments *H. pylori* supernatants 326 wild-type, 326 P9A and 326 G14A were prepared as described above; after a fourfold dilution in Dulbecco's modified Eagle's medium (DMEM) containing 2% FBS, they were administrated to the cells for the indicated time points.

Cell vacuolization assay. MEF cells (7.5×10^4 /ml) were seeded in 96-well plates in DMEM containing 10% FBS and 2 mM glutamine at 37°C in 5% CO₂ for 18 h before the assay. Cells were exposed to *H. pylori* supernatants diluted in

DMEM containing 2% FBS and 5 mM ammonium chloride. At different time points the extent of vacuolization was determined quantitatively by measuring the uptake of neutral red dye.⁴⁴ In brief, cells were incubated for 8 min in PBS 0.05% neutral red and washed three times with PBS 0.2% bovine serum albumin (BSA). After addition of 100 μ l of 70% ethanol in water containing 0.37% HCl, absorbance was measured with a Packard Fusion microplate reader (Perkin Elmer, Waltham, MA, USA) at 540 nm with subtraction of absorbance at 405 nm.

Immunofluorescence. MEF cells seeded on coverslips (2.5×10^4 /ml wild-type MEF cells seeded in 24-well plates) were transfected with the plasmid pCDNA 3.1 encoding for mtRFP; after 18 h, cells were exposed to *H. pylori* supernatants in DMEM containing 2% FBS for the indicated times. Cells were then fixed with 3.7% formaldehyde in PBS for 30 min, permeabilized with 0.01% Nonidet P40 for 20 min at room temperature and blocked with a PBS 0.5% BSA. VacA was stained with a polyclonal anti-VacA antibody⁴⁵ followed by a fluorescein isothiocyanate (FITC)-conjugated anti-rabbit secondary antibody. BAX was stained with a monoclonal anti-BAX antibody specific for the active form of the protein (clone 6A7) followed by a tetramethyl rhodamine isothiocyanate (TRITC)-conjugated anti-mouse secondary antibody. Endosomal proteins Rab5 and LBPA were labeled with monoclonal anti-Rab5 and anti-LBPA antibodies, followed by FITC anti-mouse secondary antibodies; mitochondrial protein TOM20 was labeled with a polyclonal anti-TOM20 antibody, followed by a TRITC anti-rabbit secondary antibody. In cells exposed to etoposide (Supplementary Figure 3), Rab5 was labeled with a rabbit polyclonal antibody and mitochondria were identified by a monoclonal antibody anti-complex II subunit 70 kDa. Cells were visualized with a $\times 63$ oil immersion objective on a laser-scanning confocal microscope and images were acquired using a LAS-AF software (Leica TCS-SP5, Leica Microsystems, Wetzlar, Germany). Images were then processed using ImageJ (Research Services Branch, National Institute of Mental Health, Bethesda, MD, USA) software. Mander's coefficient for colocalization analysis was calculated using Mander's coefficient plug-in of ImageJ, as previously described.⁴⁶ The quantification by Mander's colocalization coefficient was performed in a blinded manner.

Subcellular fractionation. MEF cells were seeded at the density of 10^5 /ml in 10 cm diameter tissue culture dishes and were grown in DMEM containing 10% FBS at 37°C in 5% CO₂ for 48 h. Endosomes were isolated at 4°C as described in Genisset *et al.*²⁹ In brief, cells were washed with ice-cold PBS, detached with a cell scraper and pelleted by centrifugation ($500 \times g$, 10 min). They were then washed in 3 ml of Homogenization Buffer (HB-EDTA, 0.25 M sucrose (8%) 3 mM imidazole and 0.5 mM EDTA pH 7.4), pelleted ($1300 \times g$, 10 min), resuspended in 0.7 ml of HB-EDTA and homogenized by 10 passages through a 22-gauge (1 1/4 inch) needle. After centrifugation ($1300 \times g$, 10 min), post nuclear supernatant (PNS) was collected and its sucrose concentration was increased up to 40.6% by slow addition of 62% sucrose in HB-EDTA. PNS was then carefully layered on a cushion of 1.5 ml of 35% and 1 ml of 25% sucrose in EDTA. Tubes were filled with HB, and centrifuged at 35 000 r.p.m. for 1 h at 4°C in a SW60 Ti rotor (Beckman Instruments, Fullerton, CA, USA). Late endosome-enriched fraction and early endosome-enriched fraction were collected at the interface between the 25% sucrose and HB and between the 35 and 25% sucrose, respectively.

Purified mitochondria were obtained from the nuclear pellet (NP) discharged during the purification of endosomes.³⁵ In brief, NP was re-homogenized in assay buffer (0.12 M mannitol, 0.08 M KCl, 1 mM EDTA and 20 mM K-Hepes, pH 7.4) and centrifuged at $600 \times g$. The supernatant was layered onto a cushion of 1 M mannitol in assay buffer. Tubes were filled with 2% BSA in assay buffer. After centrifugation at $9000 \times g$ for 15 min at 4°C, pellet was resuspended in 0.5 ml of assay buffer, centrifuged at $10000 \times g$ for 10 min and finally resuspended in 25 μ l of assay buffer. Protein concentration of all subcellular fractions was determined by Bradford assay.⁴⁷

To obtain the cytosolic fraction, PNS collected from 24-h-intoxicated cells was centrifuged three times at $8000 \times g$ for 10 min at 4°C as described above. Mitochondria-free supernatant was centrifuged at $100000 \times g$ for 1 h at 4°C in a 100 Ti rotor (Beckman Instruments) and the supernatant was collected as cytosolic fraction.

Immunoprecipitation, alkali extraction and immunoblotting. Co-immunoprecipitation of VacA and BAX was performed as indicated by Sawada *et al.*⁴⁸ Purified mitochondria (1 mg) were lysed in NP40 buffer (142.5 mM KCl, 5 mM MgCl₂, 1 mM EGTA, 10 mM Hepes, pH 7.4 and 0.2% Nonidet P40) supplemented with protease inhibitors (1 : 10 dilution of protease inhibitor cocktail),

After preclearing of the sample with 20 μ l protein A-Sepharose at 4°C for 2 h, lysed mitochondria were added to the beads in the presence of 4 μ g of anti-BAX polyclonal antibody. After a 16-h incubation at 4°C, beads were extensively washed with NP40 buffer plus 0.03% BSA. Proteins were finally solubilized from beads in SDS-PAGE loading buffer, before being analyzed by western blot.

For alkali extraction, early endosomes purified from cells incubated with *H. pylori* wt CS for 24 h were exposed to alkali treatment as described.⁴⁹ In brief, early endosomes were centrifuged at 100 000 $\times g$ for 1 h at 4°C in a 100 Ti rotor (Beckman Instruments) and 15 μ g was resuspended in 1 ml of 100 mM Na₂CO₃ pH 11.5, incubated for 30 min on ice, and centrifuged at 100 000 $\times g$ for 1 h at 4°C. The supernatant, containing alkali solubilized proteins, was collected and neutralized by HCl 1 M. Pellet, containing membrane integral proteins, was solubilized and proteins in both fractions were separated by SDS-PAGE and analyzed by western blot.

For immunoblotting, the following antibodies were used: anti-EEA1, LAMP1 BAX, VacA, TOM20 and COX II (dilution 1:1000). Antibodies anti-EEA1 and LAMP1 were used instead of anti-Rab5 and LBPA (applied in immunofluorescence) for identifying early endosomal and late endosomal fractions, respectively, because the quality of the signals was significantly improved.

Genetic correction of DKO MEF cells. Genetic correction of DKO SERCA and mtBAX DKO MEF cells was described in Scorrano et al.³⁰ GFP-BAX was reconstituted into *Bax* and *Bak* doubly deficient MEFs using an MSCV retroviral vector (Clontech, Mountain View, CA, USA). Stable clones expressing BAX-fusion protein were generated by limiting dilution. Full-length murine BAX was fused with an 11 amino acid N-terminal hemagglutinin (HA) tag to generate HA-BAX. Mitochondria-targeted HA-BAX (mtBAX) was constructed by fusing the 29 amino acid mitochondrial-targeted sequence from subunit VIII of human cytochrome c oxidase (COX VIII) onto the N-terminal end of HA-BAX and was present on the outer mitochondrial membrane surface. Full-length rabbit SERCA-2 and mtBAX were cloned into pcDNA3 for transient expression experiments and into a retroviral vector (MFIG) containing loxP-flanked green fluorescence protein (GFP) preceded by an internal ribosomal entry site (IRES) for stable expression. Stable clones were established by limiting dilution and were selected on the basis of GFP expression by FACS analysis. Protein expression levels of gene products were confirmed by immunoblot.

Measurement of cell death. MEF cells were incubated with the phosphatidylserine-binding protein Annexin-V conjugated to Alexa 568 (Bender MedSystem, Burlingame, CA, USA) according to the manufacturer's instructions. Viability was measured by flow cytometry (FACSCalibur, BD Biosciences, San Jose, CA, USA) as the percentage of Annexin-V-negative events in the gated population. For the viability evaluation of genetically corrected DKO MEF cells (SERCA or mtBAX) the percentage of Annexin-V-negative events was performed in the GFP-positive gated population.

Electron microscopy. Immunoelectron microscopy was performed according to the conventional protocol of Tokuyasu⁵⁰ and adapted by Slot and Geuze.⁵¹ MEF cells were fixed with 2% paraformaldehyde and 0.2% glutaraldehyde in PBS for 2 h at room temperature, embedded in 12% gelatin and cooled at 4°C for 10 min. Convenient blocks were cut and infiltrated in 2.3 M sucrose overnight and then frozen in liquid nitrogen. Ultrathin cryosections (60 nm) were cut and picked up in 1:1 2.3 M sucrose and 2% methylcellulose. Cryosections were immediately immunolabeled for LBPA with mouse anti-LBPA (dilution 1:20), and detected with a rabbit anti-mouse antibody and Protein A gold 15 nm as previously described.⁴⁸

Statistical analysis. Data were expressed as mean values \pm S.D.. Student's *t*-test was used for statistical analysis of differences between *H. pylori* wt CS-treated cells versus P9A or G14A *H. pylori* CS-intoxicated cells/untreated cells. A *P*-value of ≤ 0.05 was considered as significant.

Conflict of interest

The authors declare no conflict of interest.

Acknowledgements. This work was supported by the Italian Ministry of University and Research, Progetto di Eccellenza Fondazione Cassa di Risparmio di Padova e Rovigo, research grant by University of Padova (CPDA074121/07), Fondazione Berlucci, Associazione Italiana per la Ricerca sul Cancro grant

regionale (to MDB). FC was supported by the Graduate Academy of the EuroPathoGenomics Network of the Sixth Framework Programme of the European Community. LS is a senior telethon scientist of the Dulbecco-Telethon Institute and research in his lab is supported by Telethon Italy, Compagnia di San Paolo Italy, AIRC Italy. EM studies were performed at the Telethon Facility for Electron Microscopy, Genova, Italy (Grant GTF07002). We thank Tullio Pozzan for his critical reading and helpful suggestions.

1. Suerbaum S, Michetti P. *Helicobacter pylori* infection. *N Engl J Med* 2002; **347**: 1175–1186.
2. Leunk RD, Johnson T, David BC, Kraft WG, Morgan DR. Cytotoxic activity in broth-culture filtrates of *Campylobacter pylori*. *J Med Microbiol* 1988; **26**: 93–99.
3. D'Elios MM, Montecucco C, de Bernard M. VacA and HP-NAP, Ying and Yang of *Helicobacter pylori*-associated gastric inflammation. *Clin Chim Acta* 2007; **381**: 32–38.
4. Cover TL, Blanke SR. *Helicobacter pylori* VacA, a paradigm for toxin multifunctionality. *Nat Rev Microbiol* 2005; **3**: 320–332.
5. Tombola F, Carlesso C, Szabó I, de Bernard M, Reyrt JM, Telford JL et al. *Helicobacter pylori* vacuolating toxin forms anion-selective channels in planar lipid bilayers: possible implications for the mechanism of cellular vacuolation. *Biophys J* 1999; **76**: 1401–1409.
6. Ye D, Blanke SR. Mutational analysis of the *Helicobacter pylori* vacuolating toxin amino terminus: identification of amino acids essential for cellular vacuolation. *Infect Immun* 2000; **68**: 4354–4357.
7. McClain MS, Iwamoto H, Cao P, Vinion-Dubiel AD, Li Y, Szabo G et al. Essential role of a GXXXG motif for membrane channel formation by *Helicobacter pylori* vacuolating toxin. *J Biol Chem* 2003; **278**: 12101–12108.
8. Szabó I, Brutsche S, Tombola F, Moschioni M, Satin B, Telford JL et al. Formation of anion-selective channels in the cell plasma membrane by the toxin VacA of *Helicobacter pylori* is required for its biological activity. *EMBO J* 1999; **18**: 5517–5527.
9. Molinari M, Galli C, Norais N, Telford JL, Rappuoli R, Luzio JP et al. Vacuoles induced by *Helicobacter pylori* toxin contain both late endosomal and lysosomal markers. *J Biol Chem* 1997; **272**: 25339–25344.
10. Molinari M, Galli C, de Bernard M, Norais N, Ruyschaert JM, Rappuoli R et al. The acid activation of *Helicobacter pylori* toxin VacA: structural and membrane binding studies. *Biochem Biophys Res Commun* 1998; **248**: 334–340.
11. Gauthier NC, Monzo P, Gonzalez T, Doye A, Oldani A, Gounon P et al. Early endosomes associated with dynamic F-actin structures are required for late trafficking of *H. pylori* VacA toxin. *J Cell Biol* 2007; **177**: 343–354.
12. Jones NL, Shannon PT, Cutz E, Yeger H, Sherman PM. Increase in proliferation and apoptosis of gastric epithelial cells early in the natural history of *Helicobacter pylori* infection. *Am J Pathol* 1997; **151**: 1695–1703.
13. Mannick EE, Bravo LE, Zarama G, Realpe JL, Zhang XJ, Ruiz B et al. Inducible nitric oxide synthase, nitrotyrosine, and apoptosis in *Helicobacter pylori* gastritis: effect of antibiotics and antioxidants. *Cancer Res* 1996; **56**: 3238–3243.
14. Moss SF, Calam J, Agarwal B, Wang S, Holt PR. Induction of gastric epithelial apoptosis by *Helicobacter pylori*. *Gut* 1996; **38**: 498–501.
15. Rudi J, Kuck D, Strand S, von Herbay A, Mariani SM, Krammer PH et al. Involvement of the CD95 (APO-1/Fas) receptor and ligand system in *Helicobacter pylori*-induced gastric epithelial apoptosis. *J Clin Invest* 1998; **102**: 1506–1514.
16. Correa P, Houghton J. Carcinogenesis of *Helicobacter pylori*. *Gastroenterology* 2007; **133**: 659–672.
17. Peek Jr RM, Vaezi MF, Falk GW, Goldblum JR, Perez-Perez GI, Richter JE et al. Role of *Helicobacter pylori* cagA(+) strains and specific host immune responses on the development of premalignant and malignant lesions in the gastric cardia. *Int J Cancer* 1999; **82**: 520–524.
18. Kawahara T, Teshima S, Kuwano Y, Oka A, Kishi K, Rokutan K. *Helicobacter pylori* lipopolysaccharide induces apoptosis of cultured guinea pig gastric mucosal cells. *Am J Physiol Gastrointest Liver Physiol* 2001; **281**: G726–G734.
19. Cover TL, Krishna US, Israel DA, Peek Jr RM. Induction of gastric epithelial cell apoptosis by *Helicobacter pylori* vacuolating cytotoxin. *Cancer Res* 2003; **63**: 951–957.
20. Boquet P, Ricci V, Galmiche A, Gauthier NC. Gastric cell apoptosis and *H. pylori*: has the main function of VacA finally been identified?. *Trends Microbiol* 2003; **11**: 410–413.
21. Danial NN, Kormsmeier SJ. Cell death: critical control points. *Cell* 2004; **116**: 205–219.
22. Kimura M, Goto S, Wada A, Yahiro K, Nidome T, Hatakeyama T et al. Vacuolating cytotoxin purified from *Helicobacter pylori* causes mitochondrial damage in human gastric cells. *Microb Pathog* 1999; **26**: 45–52.
23. Galmiche A, Rassow J, Doye A, Cagnol S, Chambard JC, Contamin S et al. The N-terminal 34 kDa fragment of *Helicobacter pylori* vacuolating cytotoxin targets mitochondria and induces cytochrome c release. *EMBO J* 2000; **19**: 6361–6370.
24. Willhite DC, Blanke SR. *Helicobacter pylori* vacuolating cytotoxin enters cells, localizes to the mitochondria, and induces mitochondrial membrane permeability changes correlated to toxin channel activity. *Cell Microbiol* 2004; **6**: 143–154.
25. Willhite DC, Cover TL, Blanke SR. Cellular vacuolation and mitochondrial cytochrome c release are independent outcomes of *Helicobacter pylori* vacuolating cytotoxin activity that are each dependent on membrane channel formation. *J Biol Chem* 2003; **278**: 48204–48209.

26. Blanke SR. Micro-managing the executioner: pathogen targeting of mitochondria. *Trends Microbiol* 2005; **13**: 64–71.
27. Yamasaki E, Wada A, Kumatori A, Nakagawa I, Funao J, Nakayama M et al. *Helicobacter pylori* vacuolating cytotoxin induces activation of the proapoptotic proteins Bax and Bak, leading to cytochrome c release and cell death, independent of vacuolation. *J Biol Chem* 2006; **281**: 11205–11209.
28. Wei MC, Zong WX, Cheng EH, Lindsten T, Panoutsakopoulou V, Ross AJ et al. Proapoptotic BAX and BAK: a requisite gateway to mitochondrial dysfunction and death. *Science* 2001; **292**: 727–730.
29. Genisset C, Puhar A, Calore F, de Bernard M, Dell'Antone P, Montecucco C. The concerted action of the *Helicobacter pylori* cytotoxin VacA and of the v-ATPase proton pump induces swelling of isolated endosomes. *Cell Microbiol* 2007; **9**: 1481–1490.
30. Scorrano L, Oakes SA, Opferman JT, Cheng EH, Sorcinelli MD, Pozzan T et al. BAX and BAK regulation of endoplasmic reticulum Ca²⁺: a control point for apoptosis. *Science* 2003; **300**: 135–139.
31. Lytton J, Zarain-Herzberg A, Periasamy M, MacLennan DH. Molecular cloning of the mammalian smooth muscle sarco(endo)plasmic reticulum Ca²⁺-ATPase. *J Biol Chem* 1989; **264**: 7059–7065.
32. Wolter KG, Hsu YT, Smith CL, Nechushtan A, Xi XG, Youle RJ. Movement of Bax from the cytosol to mitochondria during apoptosis. *J Cell Biol* 1997; **139**: 1281–1292.
33. Goping IS, Gross A, Lavoie JN, Nguyen M, Jemmerson R, Roth K et al. Regulated targeting of BAX to mitochondria. *J Cell Biol* 1998; **143**: 207–215.
34. Nechushtan A, Smith CL, Hsu YT, Youle RJ. Conformation of the Bax C-terminus regulates subcellular location and cell death. *EMBO J* 1999; **18**: 2330–2341.
35. Ouasti S, Matarrese P, Paddon R, Khosravi-Far R, Sorice M, Tinari A et al. Death receptor ligation triggers membrane scrambling between Golgi and mitochondria. *Cell Death Differ* 2007; **14**: 453–461.
36. Terebiznik MR, Raju D, Vázquez CL, Torbrick K, Kulkarni R, Blanke SR et al. Effect of *Helicobacter pylori*'s vacuolating cytotoxin on the autophagy pathway in gastric epithelial cells. *Autophagy* 2009; **5**: 370–379.
37. García-Ruiz C, Colell A, Morales A, Calvo M, Enrich C, Fernández-Checa JC. Trafficking of ganglioside GD3 to mitochondria by tumor necrosis factor- α . *J Biol Chem* 2002; **277**: 36443–36448.
38. Sheftel AD, Zhang AS, Brown C, Shirihai OS, Ponka P. Direct interorganellar transfer of iron from endosome to mitochondrion. *Blood* 2007; **110**: 125–132.
39. Aslan JE, Thomas G. Death by committee: organellar trafficking and communication in apoptosis. *Traffic* 2009; **10**: 1390–1404.
40. Motyl T, Gajkowska B, Ploszaj T, Wareski P, Skierski J, Zimowska W. Expression and subcellular redistribution of Bax during TGF- β 1-induced programmed cell death of HC11 mouse mammary epithelial cells. *Cell Mol Biol (Noisy-le-grand)* 2000; **46**: 175–185.
41. Lovell JF, Billen LP, Bindner S, Shamas-Din A, Fradin C, Leber B et al. Membrane binding by tBid initiates an ordered series of events culminating in membrane permeabilization by Bax. *Cell* 2008; **135**: 1074–1084.
42. Marchetti M, Aricò B, Burroni D, Figura N, Rappuoli R, Ghiara P. Development of a mouse model of *Helicobacter pylori* infection that mimics human disease. *Science* 1995; **267**: 1655–1658.
43. Skibinski DA, Genisset C, Barone S, Telford JL. The cell-specific phenotype of the polymorphic vacA midregion is independent of the appearance of the cell surface receptor protein tyrosine phosphatase beta. *Infect Immun* 2006; **74**: 49–55.
44. Cover TL, Blaser MJ. Purification and characterization of the vacuolating toxin from *Helicobacter pylori*. *J Biol Chem* 1992; **267**: 10570–10575.
45. de Bernard M, Aricò B, Papini E, Rizzuto R, Grandi G, Rappuoli R et al. *Helicobacter pylori* toxin VacA induces vacuole formation by acting in the cell cytosol. *Mol Microbiol* 1997; **26**: 665–674.
46. De Brito O, Scorrano L. Mitofusin 2 tethers endoplasmic reticulum to mitochondria. *Nature* 2008; **456**: 605–610.
47. Bradford MM. A rapid and sensitive method for the quantitation of microgram quantities of protein utilizing the principle of protein-dye binding. *Anal Biochem* 1976; **72**: 248–254.
48. Sawada M, Sun W, Hayes P, Leskov K, Boothman DA, Matsuyama S. Ku70 suppresses the apoptotic translocation of Bax to mitochondria. *Nat Cell Biol* 2003; **5**: 320–329.
49. Komada M, Masaki R, Yamamoto A, Kitamura N. Hrs, a tyrosine kinase substrate with a conserved double Zinc finger domain is localized to the cytoplasmic surface on early endosomes. *J Biol Chem* 1997; **272**: 20538–20544.
50. Tokuyasu KT. A technique for ultracytometry of cell suspensions and tissues. *J Cell Biol* 1973; **57**: 551–565.
51. Slot JW, Geuze HJ. Cryosectioning and immunolabeling. *Nat Protoc* 2007; **2**: 2480–2491.

Supplementary Information accompanies the paper on Cell Death and Differentiation website (<http://www.nature.com/cdd>)